Investigation of the Resolution Requirements for a Hybrid RANS/LES Simulation of a Multi-element Airfoil

S. Reuß, T. Knopp, and D. Schwamborn

Deutsches Zentrum für Luft- und Raumfahrt,
Center for Computer Applications in AeroSpace Science and Engineering $C^2A^2S^2E$,
Institute of Aerodynamics and Flow Technology,
Bunsenstrasse 10,
37073 Goettingen
silvia.reuss@dlr.de

Abstract. This work is dedicated to the investigation of the resolution requirements for hybrid RANS/LES simulations for aerodynamic flows at high-lift. First, results of a local DDES for a limited section of a high-lift wing with deployed slats and flaps of a full-aircraft configuration are presented. Based on the resolution of this simulation the computational effort for a hybrid RANS/LES simulation of the complete high-lift wing is estimated. Since this estimate results in prohibitively high costs, the focus is shifted to the scale-resolving simulation of a quasi two-dimensional segment of a three-element wing for the further investigations. Three approaches, a zonal DDES, a global DDES and an IDDES, are presented and the last one is evaluated with respect to the resolution of the boundary layers as well as the free shear layers.

1 Introduction

The idea of hybrid RANS/LES models is to reduce the computational effort compared to a pure LES computation by treating attached boundary layers in RANS mode. RANS models are reliable if applied to attached flows with a small or moderate pressure gradient, while hybrid models like the Detached Eddy Simulation (DES) model [1] have been applied with great success to test cases with massive separation, fixed by the geometry. In these cases a clear superiority over RANS models has been demonstrated [2]. Flows with smaller separation, caused by an adverse pressure gradient, are still very challenging for the numerical simulation. The benefit of hybrid RANS/LES models for these cases is under investigation.

The reduction of airframe-noise caused by the high-lift devices is one important contribution to the reduction of the overall noise of an aircraft. The direct access to the instationary sources of aerodynamic noise is another motivation for a hybrid RANS/LES simulation.

N. Kroll et al. (eds.), *Computational Flight Testing*, Notes on Numerical Fluid Mechanics and Multidisciplinary Design 123,
DOI: 10.1007/978-3-642-38877-4_4,

When the ComFliTe project was started, the idea was to assess a local hybrid RANS/LES approach for a section of a high-lift wing of a full-aircraft in landing configuration near maximal lift $C_{l,max}$. At this point there were several open questions:

1. What are the expected computational costs for such a simulation?
2. Which model from the DES family is best suited for high-lift cases?
3. Which requirements for a proper mesh resolution can be given?

The outline of this paper is as follows: In Sec. 2 the numerical method is shortly described. In Sec. 3 results from a local DDES of a section of a high-lift wing with a small spanwise extent embedded into a global RANS simulation of a full-aircraft configuration with focus on the aeroacoustics in the slat cove are presented. These are used in Sec. 4 to estimate the computational effort for a local DDES for the complete high-lift wing. With this estimate an answer to the first question could be given: it is not feasible to perform a zonal DDES for a complete high-lift wing of a full-aircraft configuration with the currently available computing resources and the budget within the ComFliTe project. Therefore, in order to find answers to the remaining open questions, the focus of the work was redefined and a three-element airfoil with periodic boundary conditions in the span-wise direction was chosen as the new test case. This configuration is described in Sec. 5. The results from several hybrid simulations are shown in Sec. 6 and the evaluation of the grid resolution is presented in Sec. 7. In the last section conclusions are drawn and an outlook is given.

2 Numerical Method

All simulations were performed with the DLR TAU code [16], a compressible finite volume solver for the Navier-Stokes equations on unstructured meshes. The time-accurate simulations employ a dual time-stepping scheme with a three-stage low-storage Runge-Kutta scheme. The spatial discretization uses a central scheme with artificial dissipation of matrix type. The convergence is accelerated by a 3w multi-grid scheme. Different turbulence models are implemented for the closure of the Reynolds-Averaged NS-equations and based on these RANS models different variants of the hybrid RANS/LES models are available. The different variants can be distinguished by the function that switches from RANS to LES. In the original DES model [1] the switching is based on the size of the grid cells, whereas the Delayed DES (DDES) [4] variant provides a shielding function that is designed to ensure the RANS mode in the whole boundary layer independent of the grid. The Improved DDES (IDDES) [5] model additionally offers a mode that allows for wall modeled LES, resolving the outer part of the boundary layer.

All hybrid simulations that are presented here, are based on the Spalart-Allmaras turbulence model, utilizing the DDES as well as the IDDES model.

3 Local DDES of a High-Lift Wing

The full-aircraft configuration is a model of the A320 wing-body with nacelles and deployed slats and flaps. The wind-tunnel model has a half span width of 1.08 m and a mean chord length of $c_{mean} = 0.224$ m. Experiments were performed at a Mach number of $Ma = 0.2$ and a Reynolds number of $Re = 1.34 \times 10^6$ at an angle of attack of $\alpha = 4°$. The experimental data for this test case were obtained within the research project HICON [6]. One of the objectives of the project was to reduce the noise emissions of aircraft through innovative high-lift configurations. Therefore, the spectra emitted by the high-lift devices of a wind-tunnel model of an A320 were measured with microphone arrays. Additionally, the mean pressure distributions were taken in several span-wise positions.

The objective of the numerical investigation was to assess the influence of the model slat tracks on the emitted spectra. Therefore, a single model slat track, located at 60% span width, was included in the geometry. The aim of this work was to compare the noise that is generated by the model slat track to the noise that is emitted by a real slat track.

In order to obtain information about the instationary sources of noise, a local DDES was performed: the scale-resolving approach was used in the vicinity of the slat track while in the major part of the computational domain the RANS approach was used. To provide a mesh for this zonal approach, an appropriate hybrid grid for a RANS simulation with about 30×10^6 points was used as a basis. This basic mesh was refined in a region around the track of about 7% span-wise extent. The refined grid consisted of 80×10^6 points, with all additional 50×10^6 points located in the focus region, the wake of the slat track. A view of the region with the model slat track is presented in Fig. 1. The dark area on the main wing indicates the surface of the refined region for the zonal approach.

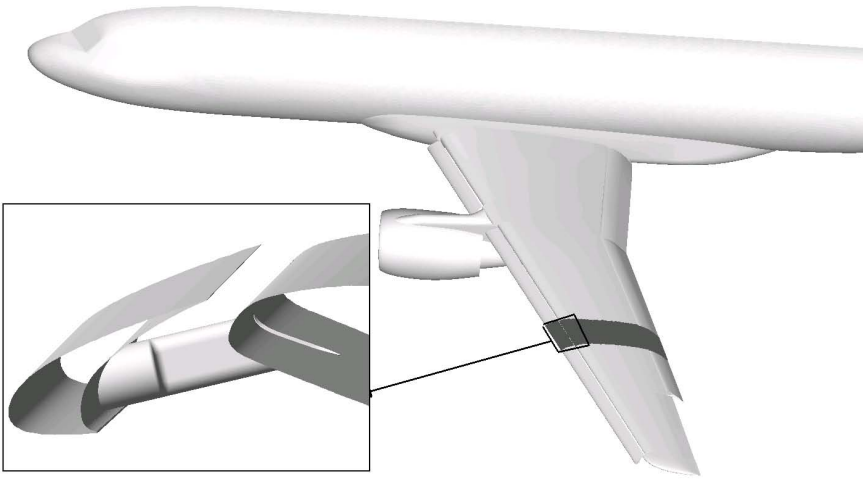

Fig. 1. Focus region of the local DDES of a full-aircraft configuration in high-lift with a single slat track

Spatial Resolution Requirements for the spatial resolution can be estimated by the measured frequencies: The acoustical data range from $f_0 = 2000$ Hz to $f_1 = 40,000$ Hz. With a speed of sound of about $a = 343$ m/s at a temperature of $T = 293$ K and a free-stream velocity of $u_\infty = 68$ m/s the distance that one acoustic wave travels per acoustic oszillation period is $\ell = u_\infty + a/f_1 \approx 0.01$ m. To resolve this distance appropriately about 30 points are needed. Therefore, the cell size in the focus region should be about $\Delta_x = 3.33 \times 10^{-4}$ m.

The refined grid was generated using the CENTAUR software. CENTAUR generates hybrid grids with hexahedral or prismatic cells in the near wall regions and tetrahedral cells in the farfield. The grid generation is controlled by sources that define the cell size in different regions. While on the one hand this process needs little interaction from the user, on the other hand no full controll over the shape of the elements is possible. The average cell size in the stream-wise and span-wise direction in the focus region is $\Delta_x = \Delta_y = 3.6 \times 10^{-4}$ m. The average number of surface points in a stream-wise cut through the wing is 2600. In the wall-normal direction the number of points in the structured layers is 30.

The generation of the refined grid was very time-consuming with one run lasting several days. Therefore, it was not possible to perform many iterations of the grid generation process, so that finally a compromise had to be made regarding the geometrical quality of the grid elements: unfavorable acute-angled and skewed grid cells could not be avoided completely. These can deteriorate the convergence rate of a simulation considerably, which was the case in the present simulations. So, in order to ensure an appropriate convergence per physical time step, the number of inner iterations had to be almost doubled compared to typical values from other hybrid RANS/LES simulations (e.g. those presented later on), leading to an increased computational effort for each physical time step.

Temporal Resolution The time step that is necessary for the resolution of the aeroacoustics can also be estimated from the measured frequencies. In order to resolve one period of the highest frequency of $f = 40,000$ Hz with about 30 time steps, the time-step size should be about $\Delta t_{acous} \approx 1 \times 10^{-6}$ s. A similar estimate is obtained if the time is computed as the ratio between cell size Δ_x and sum of far field velocity u_∞ and speed of sound a. However, if the focus is not on the aeroacoustics the estimate of the time step can be solely based on the free stream velocity $\Delta t = \Delta x/u_\infty \approx 5 \times 10^{-6}$ s. In order to get physically meaningful spectra several periods of the lowest frequencies must be simulated. 100 periods of the 2000 Hz frequencies would result in 0.05 s simulation time. This would all together result in 50,000 physical time steps using Δt_{acous}. However, in order to get converged mean-flow and turbulent statistics a certain number of Convective Time Units (CTU), $t_{CTU} = \ell/u_\infty$, is needed as well, where ℓ is a characteristic length of the geometry, e.g. $\ell = 0.253$ m the averaged chord length of the airfoil in the refined region. Then $t_{CTU} = 0.0037$ s is the time that it takes the flow to pass the characteristic length. In order to get accurate second order statistics, $50t_{CTU}$ are usually necessary which leads to 185,000 physical time steps using Δt_{acous}.

Parallel speedup With this large number of grid points the region of linear speedup extends to large numbers of processors. In the current case the computations were performed on 2048 cores of the DLR $C^2A^2S^2E$ cluster. At the time of the computations this was one third of the available resources of the cluster. The speed of the computation was almost doubled through doubling the number of processors.

With this massive parallel computational effort about 20 minutes of real time were needed to simulate one physical time step. Simulating 50,000 physical time steps would then have taken 694 days which was beyond the scope of the resources that could be acquired for this work. Therefore, it was decided to reduce the temporal resolution by a factor of 10. With the reduced number of required time steps of 5,000 this still lead to a real simulation time of 69 days without interruption.

A scale-resolving hybrid RANS/LES simulation starts with an initial transient phase. In this phase the generation of turbulent content builds up. This phase must be overcome before reliable statistics can be computed and it is not clear a-priori how long it lasts, but at least several convective times t_{CTU} are needed. An indicator for a fully developed turbulent flow are converged mean values.

During the simulations of the A320 some uncertainties aroused from other hybrid RANS/LES simulations of airfoil flows, that were conducted at the same time. These and limited computational resources led to the decision to stop the simulations prematurely. Even though the statistical evaluation of the results was not possible with the limited data available, still relevant insights into the computational effort of a such a scale-resolving simulation could be gained.

A representative qualitative result is presented in Fig. 2, depicting an iso-surface of the Q_{inv}-criterion:

$$Q_{inv} = \frac{1}{2}\left[|S|^2 + |\Omega|^2\right] > 0$$

with $S = \frac{1}{2}\left[\nabla \boldsymbol{u} + (\nabla \boldsymbol{u})^T\right]$ and $\Omega = \frac{1}{2}\left[\nabla \boldsymbol{u} - (\nabla \boldsymbol{u})^T\right]$, which is an indicator for a vortex, where the norm of the vorticity tensor dominates that of the rate of strain. The criterion can be used to visualize the small scale structures that form in the wake of the slat track. The span-wise velocity component v is used to demonstrate the three-dimensional nature of the structures. It can be clearly seen that the major vortical structure over the main wing originates from the slat track, which is itself not visible in the picture.

4 Estimation of the Resolution Requirements for a DDES for a Complete High-Lift Wing

In order to be able to compare the resolution for different test cases, all scales are given in percentage of the retracted chord length. In the case of the A320 the average retracted chord length in the refined region around the slat track, $c = 0.253$ m, is used. The span-wise extent of the refined mesh region is $L_y = 26\%c$. The average cell size in the stream-wise and span-wise direction in this

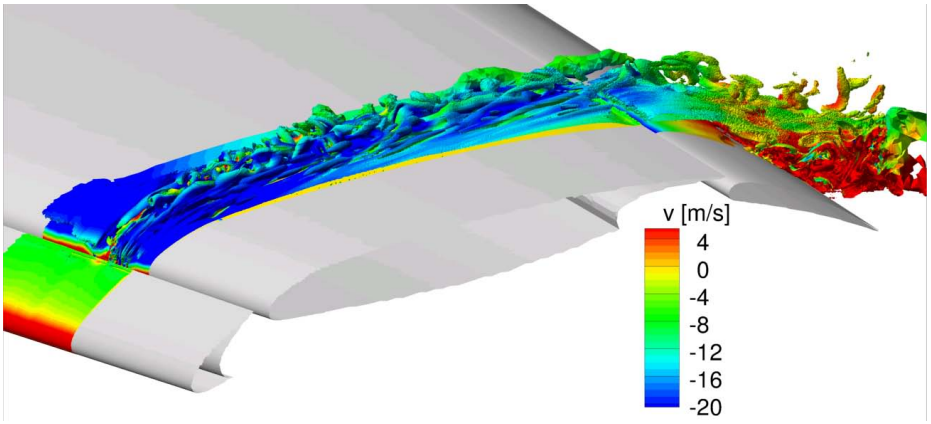

Fig. 2. Iso-surface of the Q_{inv}-criterion to visualize the turbulent structures in the wake of the slat track, colored with the span-wise velocity component v

region is $\Delta_x = \Delta_y = 0.14\%c$. Hereby, in the focus region, the number of points in span-wise direction can be roughly approximated as $L_y/\Delta_y \approx 200$. With about 50×10^6 points in total in the refined region this leaves about $N_{x,z} = 250,000$ points in one plane normal to the span-wise direction.

The resolution of the limited zonal DDES is extrapolated in order to estimate the expected computational effort of a global DDES for a similar high-lift wing configuration. The geometry has a span width of $L_{span} = 425\%c = 1.088$ m. Neglecting the span-wise variation of the chord length and using the same resolution Δ_y over the entire wing leads to a total number of points $N_y = 3000$ in the span-wise direction. If in each plane a similar resolution with $N_{x,z} = 250,000$ was used, the total number of points would be 750×10^6. In this estimation the nacelle is omitted.

Even if it were possible to avoid the geometrical difficulties described above and thus to halve the computational effort, with the estimated time step of $\Delta t = 5 \times 10^{-6}$ s (focus on aerodynamics) an overall real time of about 10 years would be necessary to simulate $50t_{CTU}$ on the same number of processors. However, this estimate is based on a grid with a very high resolution of the slat cove area, as in the zonal approach the focus was on the acoustics in this region. If the local phenomena of the high-lift devices are not resolved in particular and instead the focus of a hybrid RANS/LES simulation is on the wake of the entire airfoil, then the costs can be reduced considerably. In order to investigate the physics of the high-lift devices, the need for a test case with manageable complexity became obvious. The remedy was using a cut through a wing with deployed high-lift devices with periodic boundary conditions in the span-wise direction. This way the size of the computational domain can be decreased considerably and it is possible to focus on the local flow phenomena that are caused by the high-lift devices.

5 DLR-F15 Three-Element Airfoil: Test Case Description

The investigated DLR-F15 three-element airfoil was developed in the project LEISA as a two-dimensional cut through a generic aircraft wing with deployed slat and flap [7]. Here, experimental data at a moderate angle of attack of $\alpha = 7°$ are used, as the separation at the wind-tunnel side-walls is considered minor for low angles. Thus the flow can be regarded as almost two-dimensional and it is justified to use periodic boundary conditions in the span-wise direction in the simulations. Measurements were performed in the low-speed wind-tunnel NWB at DLR Braunschweig at a Reynolds number of $Re = 2 \times 10^6$ based on the retracted chord length and a Mach number of $Ma = 0.15$. The wind-tunnel model has a chord length of $c = 0.6$ m and a span width of 2.8 m. The experimental data used for validation consist of the mean pressure distribution in three span-wise sections and infrared measurements to locate the transition from laminar to turbulent flow. However, there are no experimental data available for the mean velocity or the Reynolds stresses.

Even though the geometrical complexity of the test case is significantly reduced, compared to the full-aircraft configuration, the accurate prediction of the physical phenomena of the flow is still very challenging: All elements produce a wake flow that interacts with the following elements. Additionally, driven by an adverse pressure gradient, the flow separates at the flap at this angle of attack. In order to capture this separation the upstream flow must be accurately predicted.

In a three-dimensional simulation the geometrical extent of the computational domain is fixed, whereas the decision about the span-wise extent of the quasi two-dimensional simulation is left to the user. Here, some guidelines can be found in [8], where the coherence of the perturbation pressure over the span-wise extent is analyzed. The authors write that the span-wise extent of the computational domain should be at least 80% of the slat chord length c_{slat} in order to allow the solution in the slat cove and on the main wing element nose to become completely de-correlated if periodic boundary conditions are used. Here, with $c_{slat} = 20\%c$ this results in a recommended span-wise extent of $16\%c$. On the other hand using twice the height of the separation region on the flap ($2.5\%c$ in the RANS simulations) is considered sufficient for the resolution of the separation. In the presented simulations a span-wise extent of $9\%c$ is chosen, to ensure sufficient resolution of the separation on the flap.

The geometrical quality of the grid elements can be easily controlled in this case: The three-dimensional grid is obtained by stacking a number of identical two-dimensional grids with constant step size in the span-wise direction (y-direction). The two-dimensional grid has also been constructed with CENTAUR and consists of about 200,000 points in the xz-plane with 2000 points on the surfaces of all three elements and 45 cells normal to the wall in the structured layers. The first node above solid walls is located at a distance of about one in plus units. The cell size in the focus region, i.e. the slat cove and in the separation region above the flap, is about $0.14\%c$. Using 64 layers of this grid in span-wise direction over a spanwise extent of $9\%c$ leads to a total number of 12.8×10^6

points. After the first DDES simulation the grid was redesigned. The number of points was not significantly changed but the resolution in the slat cove and above the flap was increased, while the resolution of the leading edges of all elements was decreased. With $\ell = 0.6$ m and a free-stream velocity of $u_\infty = 50$ m/s one convective time unit is $t_{CTU} = 0.012$ s; resolving one CTU by 600 steps the time step in the simulation was chosen as $\Delta t = 2 \times 10^{-5}$ s.

In Table 1 the spatial and temporal resolution of the A320 and the DLR-F15 test case are compared.

Table 1. Temporal and spatial resolution of the A320 and the DLR-F15 test case

	A320	DLR-F15
cell size in focus region	$0.0014c$	$0.0014c$
No. of points on surface	2600	2000
No. of wall-normal structured points	30	45
No. of points in xz-plane	250,000	200,000
time step Δt	1×10^{-5} s	2×10^{-5} s
No. of time steps per t_{CTU}	370	600

6 DLR-F15 Three-Element Airfoil: Results

Part of the following simulations were performed within the European project ATAAC [9] and a detailed presentation is given in [10]. Here only those results are repeated that are relevant to the current investigations. Three different approaches were applied: a DDES, a zonal DDES and an IDDES. Concerning the second question raised in the introduction regarding the best approach to treat multi-element airfoils the results can give a guideline: The DDES approach seems to be unable to handle the confluence of the shear layer of the slat with the boundary layer on the main-wing element. Two possibilities to handle this flaw were exploited:

1. In the confluent region the RANS mode is enforced and the transport of instabilities into the boundary layer is suppressed.
2. IDDES is used which was designed to deal with unsteadiness in boundary layers by switching into an wall modeled LES mode. Therefore, it should be an ideal candidate for the interaction between a shear layer and an underlying boundary layer, sufficient resolution in space and time provided.

In the following, snapshots of the flow are compared for the different hybrid approaches. Then the mean pressure distributions are compared with RANS results.

Vorticity. An instantaneous snapshot of the contour of the vorticity is shown in Fig. 3. This snapshot gives an impression of the large range of scales that are present in the flow.

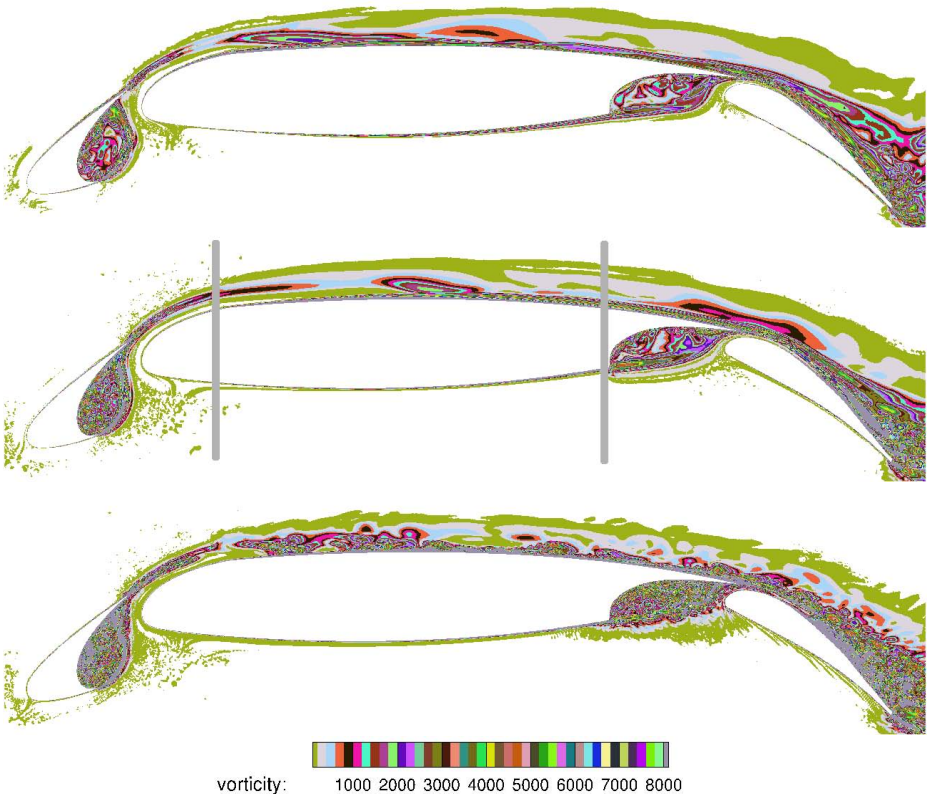

Fig. 3. Instantaneous contour of the vorticity: SA-DDES (top), zonal SA-DDES (middle) and SA-IDDES (bottom)

The vortical structures in the DDES (top) are quite coarse in the slat cove. Behind the slat trailing edge the free shear layer breaks up and the unsteady structures penetrate into the boundary layer on the main wing. This disturbance of the formal RANS layer is persistent all the way over the main wing element even very close to the wall, where a steady-state RANS solution would be expected. Associated with these unsteady events, additional turbulent kinetic energy is transported into the boundary layer and at the same time it seems that the turbulence production of the RANS model is increased, leading to massively overpredicted levels of turbulent shear stress. This shear stress is responsible for the wall-normal transport of momentum in the boundary layer. An increased shear stress also leads to a higher transport of momentum towards the wall over the flap, which prevents the separation on the flap.

In the vorticity distribution of the zonal DDES (middle), the boundaries of the enforced RANS region are indicated by the gray lines. The redesigned grid has a positive effect on the resolved structures in the slat cove. Even though the situation is formally the same as in the non-zonal DDES up to the interface of

the enforced RANS zone, the structures are much smaller than before. Once the free shear layer enters the RANS region, the vortical structures are not damped immediately. Even though the shear layer is preserved longer compared to the non-zonal DDES, it breaks up finally and again penetrates into the near wall region of the boundary layer, leading to a similar situation as in the standard DDES case on the less resolved grid.

For the IDDES (bottom) the vorticity contours show again a break up of the shear layer behind the slat. The resolved structures in the slat cove as well as above the flap are much smaller than in the zonal approach. Compared to the DDES result the vortical structures that travel along the main wing element are much smaller and they are preserved all the way to the trailing edge, indicating that the IDDES runs in WMLES mode.

Pressure Distribution. The pressure distributions of all three hybrid approaches are compared with two different Spalart-Allmaras based RANS simulations in Fig. 4. These reference RANS simulations differ in the way how the transition from laminar to turbulent flow is handled. In the first case, RANS 1, the transition is prescribed on all elements, i.e. the slat is laminar, on the main wing and flap transition locations are prescribed similar to the observed position in the infra-red measurements. In the second simulation, RANS 2, no laminar regions are prescribed on the flap. This choice has a big influence on the solution and uncertainties concerning the transition settings are transported to the hybrid simulations since it is not feasible to compare different settings for all the approaches. Therefore, the setting without laminar regions on the flap was chosen. The DDES was carried out for about $22t_{CTU}$. With this approach the flow stayed attached: in the pressure distribution no plateau can be seen at the rear

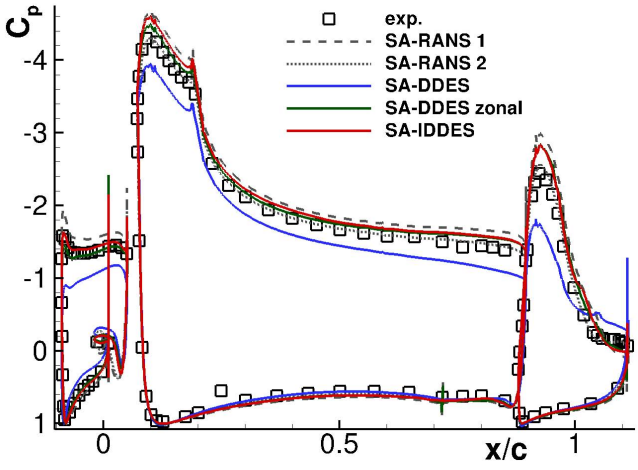

Fig. 4. Mean pressure distribution from SA RANS, DDES, zonal DDES and IDDES

of the flap. The suction peaks on all elements are too small and the pressure distribution deviates significantly from the experimental data and the RANS simulations.

In a zonal DDES the RANS mode was enforced around the main wing element. This simulation ran for about $30t_{CTU}$ and then was stopped when again no separation on the flap was observed. The pressure distribution is in better agreement with RANS and experiments than the non-zonal DDES. The missing separation on the flap leads to higher suction peaks on the slat and main wing and the plateau on the flap is not reproduced.

The IDDES was run for the longest time until statistical convergence was reached after about $100t_{CTU}$. The mean and RMS values were evaluated based on the last $40t_{CTU}$. The suction peaks in the pressure distribution are higher than in the zonal DDES simulation but a small plateau can be seen at the rear of the flap. The IDDES approach predicts separated flow on the flap.

7 DLR-F15 Three-Element Airfoil: Assessment of Resolution

The grid resolution was estimated using three different approaches. An additional RANS simulation using the Wilcox $k\omega$-model was performed. The turbulent length scale from that RANS simulation was used to evaluate the resolution in the recirculation region and in the free shear layer. A global estimate of the resolution was obtained from the comparison of the modeled and the resolved turbulent kinetic energy. The ratio of modeled to total shear stress was used to evaluate the resolution in the near wall regions.

7.1 Turbulent Length Scale

In Fig. 5, the turbulent length scale $\ell = \sqrt{k}/\omega$ that is computed from the $k\omega$-RANS simulation is shown as percentage of the chord length. The length scale in the slat cove is about $\ell = 0.07\%c$ and in the shear layer behind the slat even $\ell = 0.04\%c$. With a cell size of $0.14\%c$ in the grid the resolution is of the same order of magnitude, but little too low. With the approach of generating the three-dimensional grid by stacking two-dimensional grids in span-wise direction, a higher resolution does not seem feasible, given the computational ressources.

7.2 Ratio of Modeled to Resolved Turbulent Kinetic Energy (TKE)

In Fig. 6, the resolved TKE that is obtained in the IDDES simulation is compared with the modeled TKE predicted with the $k\omega$-RANS simulation. Above the flap the level of resolved energy is of the same order of magnitude in the two approaches. However, in the slat and wing coves the resolved TKE is higher in the IDDES. In Fig. 7 the ratio of the modeled to the total turbulent kinetic energy is shown. In the literature a value of 0.8 is taken as a threshold for a well resolved LES. This value is reached in the slat cove; however, in the wake behind the slat this estimation suggests that the wake is under-resolved.

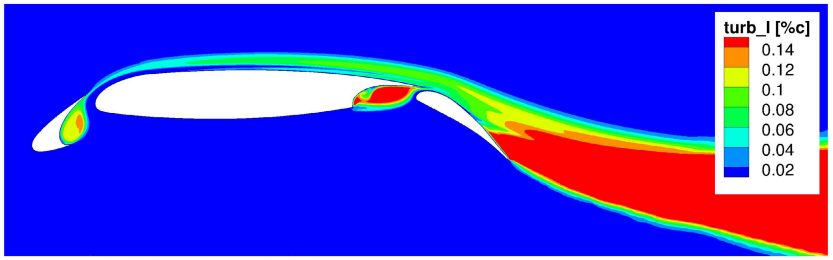

Fig. 5. Turbulent length scale ℓ from $k\omega$-RANS as percentage of the chord length

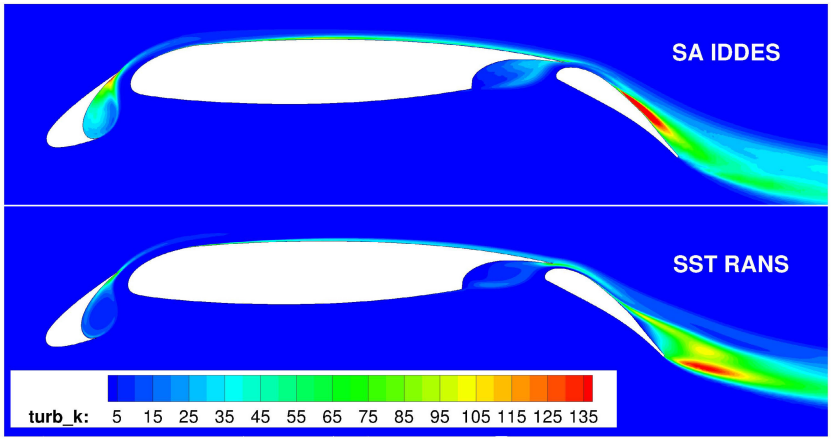

Fig. 6. Turbulent kinetic energy (in m^2/s^2) from SA-IDDES (top) and from $k\omega$-RANS (bottom)

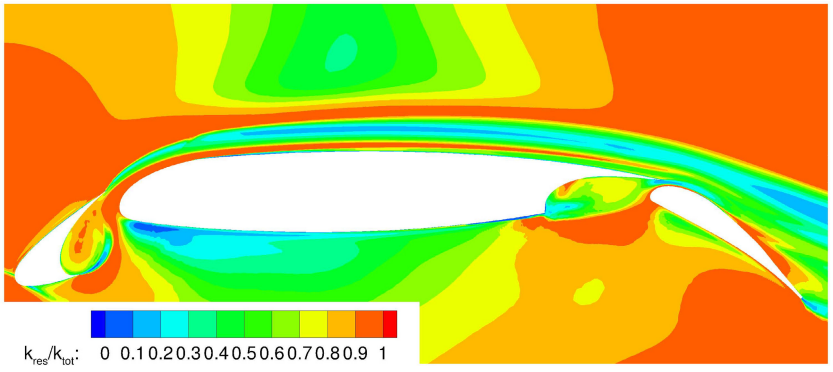

Fig. 7. Ratio of resolved TKE to total TKE in the SA-IDDES

7.3 Ratio of Modeled to Resolved Shear Stress

The total turbulent shear stress is given by

$$(\tau_{xz})^{turb}_{total} = \underbrace{\mu_t \left(\frac{du}{dz} + \frac{dw}{dx} \right)}_{(\tau_{xz})^{turb}_{modelled}} - \underbrace{\rho \langle u'w' \rangle}_{(\tau_{xz})^{turb}_{resolved}} \quad .$$

In Fig. 8 the ratio of the modeled to the resolved shear stress in the IDDES on the upper side of the main wing element is shown. The thick solid line indicates the edge of the boundary layer, estimated by the $\Xi = y|du/dy|$ criterion of Stock and Haase [11]. The dashed line indicates a value of the hybrid switch function $f_d = 0.95$ and thus the edge of the formal RANS region of the hybrid approach. Here it can be seen, that the whole formal RANS region is treated in the RANS mode since the modeled stress is larger than the resolved stress. To further estimate the resolution in the outer part of the boundary layer, the ratio of the averaged velocity fluctuations in the stream-wise and the wall-normal direction is shown in Fig. 9. In an under-resolved LES artificially large streaks in the stream-wise direction can be observed [12]. These structures can be identified and characterized by a large anisotropy in the ratio of the stream-wise to the wall-normal velocity fluctuations. In a well resolved LES a ratio of about 1.5 is expected [13]. Here, the ratio is about 8 in the outer part of the boundary layer indicating an under-resolved LES. Finally the resolution in the wake behind the slat trailing edge is estimated using the same approach. The ratio of the

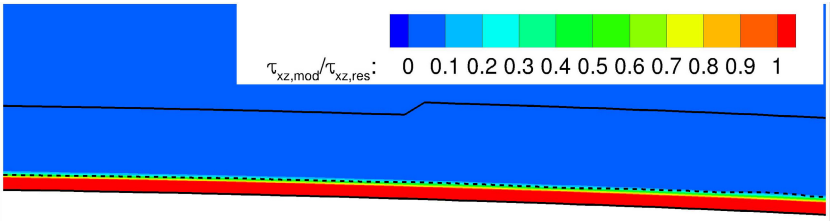

Fig. 8. Ratio of modeled to resolved shear stress on the upper side of the main wing element in the IDDES

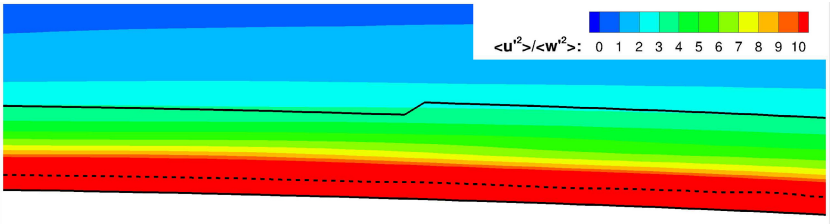

Fig. 9. Ratio of resolved velocity fluctuations in stream-wise and wall-normal direction on the upper side of the main wing element in the IDDES

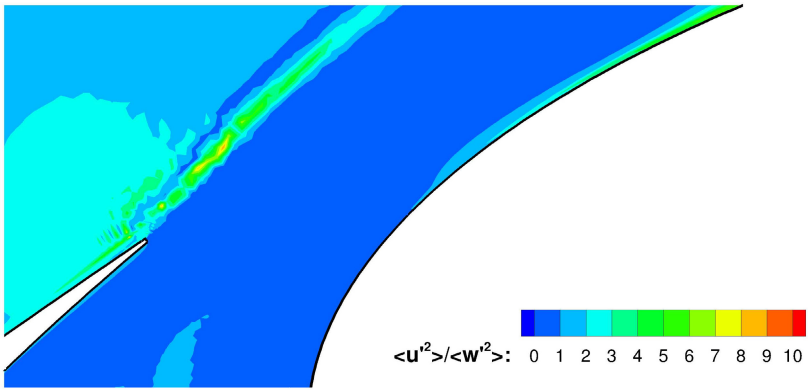

Fig. 10. Ratio of resolved velocity fluctuations in the stream-wise and the wall-normal direction in the wake behind the slat trailing edge in the IDDES

stream-wise to the wall-normal velocity fluctuations, shown in Fig. 10, takes values between 4 and 9 in a part of the wake. This indicates again that a higher resolution of the wake would be needed.

8 Conclusions and Outlook

Results of a zonal DDES of a A320 wing-body configuration with deployed slat and flap were presented. The focus of this simulation was on the acoustics in the slat-cove. Even for this zonal approach it was not possible to achieve converged mean flow and turbulent statistics. However, conclusions regarding the computational effort of such a simulation could be drawn. The presented results were used to estimate the computational effort of a global DDES simulation for a similar configuration and it could be stated that this simulation would not be possible within the framework of the ComFliTe project.

As a consequence, the DLR-F15 three-element airfoil was chosen as the further test case and three hybrid approaches were tested: zonal DDES, global DDES and IDDES. Instantaneous snapshots of the vorticity were compared for all approaches and it was found, that the DDES is not able to handle the confluence of the free shear layer behind the slat with the attached boundary layer on the main wing. Enforcing the RANS mode in the region of confluence in the zonal approach is not sufficient, if no additional means are taken to damp the resolved structures in the free shear layer. With both approaches, zonal and global DDES, the separation on the flap was suppressed through this improper representation of the confluence through the hybrid model. One possibility would be to use a much coarser grid in the enforced RANS region in the zonal approach in order to increase the numerical dissipation and damp the LES solution. This approach could be recommended from an engineering point of view if the focus of a simulation is on local features while unsteady features in other regions can remain unresolved.

The IDDES approach, however, was able to predict the separation on the flap. This demonstrates that this approach is able to handle the interaction of the slat wake with the boundary layer on the main wing in a physically correct way. However, the evaluation of the data indicates that the flow was still under-resolved, which leads to the conclusion that the IDDES approach is very promising, but that a very highly resolved grid is needed.

Acknowledgment. The authors are very grateful to their colleague S. Melber-Wilkending from the transport aircraft branch of the DLR institute of aerodynamics and flow technology for providing the basic RANS grid for the zonal DDES of the A320 and to the colleagues J. Wild and M. Pott-Pollenske for the assistance regarding the aeroacoustic questions. We also thank Airbus for funding this work and providing the experimental data for the A320 test case.

References

1. Spalart, P.R., Jou, W.H., Strelets, M.K., Allmaras, S.R.: Comments on the feasibility of LES for wings, and on a hybrid RANS/LES approach. In: 1. AFOSR Int. Conf. Advances in DNS/LES, August 4-8 (1997)
2. Notes on Numerical Fluid Mechanics and Multidisciplinary Design, Vol. 103: DESider A European Effort on Hybrid RANS-LES Modelling (2009)
3. Schwamborn, D., Gardner, A., von Geyr, H., Krumbein, A., Lüdeke, H., Stürmer, A.: Development of the TAU-Code for aerospace applications. In: 50th NAL International Conference on Aero-space Science and Technology (2008), `http://www.nal.res.in/nal50/incast/incast/01-Invited`
4. Spalart, P.R., Deck, S., Shur, M.L., Squires, K.D., Strelets, M.K., Travin, A.: A New Version of Detached-eddy Simulation, Resistant to Ambiguous Grid Densities. Theoretical and Computational Fluid Dynamics 20(3), 181–195 (2006)
5. Shur, M.L., Spalart, P.R., Strelets, M.K., Travin, A.: A hybrid RANS-LES approach with delayed-DES and wall-modelled LES capabilities. International Journal of Heat and Fluid Flow 29(6), 1638–1649 (2008)
6. Sutcliffe, M., Reckzeh, D., Fischer, M.: HICON Aerodynamics - High Lift a aerodynamic design for the future. In: 25th International Congress of the Aeronautical Sciences ICAS (2006)
7. Wild, J., Pott-Pollenske, M.: An integrated design approach for low noise exposing high-lift devices. AIAA Paper 2006-2834 (2006)
8. Lockard, D.P., Choudhari, M.M.: Noise Radiation from a Leading-Edge Slat. AIAA Paper 2009-3101 (2009)
9. `http://cfd.mace.manchester.ac.uk/ATAAC/WebHome`
10. Reuß, S., Knopp, T., Schwamborn, D.: Hybrid RANS/LES simulations of a three element airfoil. Notes on Numerical Fluid Mechanics and Multidisciplinary Design, vol. 117: Progress in Hybrid RANS-LES Modelling (2012)
11. Stock, H.W., Haase, W.: The Determination of Turbulent Length Scales in Algebraic Turbulence Models for Attached and Slightly Separated Flows Using Navier-Stokes Methods. In: AIM 19th Fluid Dynamics, Plasma Dynamics and Lasers Conference, AIAA Paper 1987-1302 (1987)
12. Piomelli, U., Balaras, E.: Wall-Layer Models for Large-Eddy Simulations. Annual Review of Fluid Mechanics (34), 349–374 (2002)
13. Pope, S.B.: Turbulent Flows. Cambridge University Press (2000)